


Impact of Ga and N Vacancies at the GaN m -Plane on the Carrier Dynamics of Micro-Light-Emitting Diodes

Purun-hanul Kim¹, Sang Ho Jeon², Jin Hyuk Jang², Seungwu Han¹, and Youngho Kang^{3,*}

¹*Department of Materials Science and Engineering and Research Institute of Advanced Materials, Seoul National University, Seoul 08826, Korea*

²*Display Research Center, Samsung Display Co. Ltd., Yongin-si, Gyeonggi-do 17113, Korea*

³*Department of Materials Science and Engineering, Incheon National University, Incheon 22012, Korea*

 (Received 30 August 2022; revised 11 November 2022; accepted 12 December 2022; published 6 January 2023)

Micro-light-emitting diodes (μ LEDs) based on GaN are a key component for next-generation displays, but serious surface e - h recombination deteriorates the device efficiency. To gain microscopic insights into the surface recombination, we use hybrid functional first-principles calculations to investigate Ga (V_{Ga}) and N (V_{N}) vacancies on the GaN m plane that can be created considerably during the production of one-dimensional GaN structures. We find that the surface V_{Ga} is not critical for nonradiative Shockley-Read-Hall (SRH) recombination in light of the large formation energy (>2 eV) and its shallow levels. In contrast, the surface V_{N} exhibits a low formation energy (<2 eV) and develops a deep defect state near the midgap, indicating the possibility of becoming useful SRH recombination centers. By constructing configuration-coordinate diagrams, we demonstrate that the energy barriers for electron and hole capture on the surface V_{N} are small enough to cause significant capture coefficients due to strong electron-phonon coupling.

DOI: [10.1103/PhysRevApplied.19.014018](https://doi.org/10.1103/PhysRevApplied.19.014018)

I. INTRODUCTION

Over the last few decades, liquid-crystal displays (LCDs) and organic light-emitting diodes (OLEDs) have been the mainstream display technologies. These two technologies have their own advantages: LCDs have low cost, high durability, and high power efficiency [1] and OLEDs have self-emission and high contrast [2–4]. However, with the recent advances in mobile devices such as smartphones, laptops, and tablets as well as televisions (TVs), the demand for high-performance displays with specs that are not easily met by using LCDs and OLEDs has grown rapidly. For instance, LCDs are not suitable for developing self-emitting displays with large areas, fast responses, and high contrast [5], while OLED-based displays often suffer from various degradation issues related to material instability [6]. In addition, for augmented reality (AR) and virtual reality (VR) effects that are emerging in the display technology of our present hyperconnected society, an ultrahigh density of more than 3000 pixels per inch (PPI) is needed to eliminate the screen-door effect [5]. However, it is challenging to achieve such high pixel densities using the present LCD and OLED technologies because of several limitations in production processes, e.g., a lack of relevant back-plane processes for the former and an

absence of precise deposition techniques that can prevent the degradation of devices and materials for the latter [7,8].

Owing to their high efficiency and versatility, light-emitting diodes (LEDs) based on GaN and its alloys have been used extensively for solid-state lighting over the last three decades [9–14]. Recently, micro-sized LEDs (μ LEDs) have garnered a great deal of attention as promising technologies for next-generation display applications because μ LEDs can have the advantages of low power consumption, self-emission, and high contrast [15–18]. Furthermore, the micrometer dimension of μ LED enables pixel densities over a few thousand PPI that are large enough to create AR and VR displays [18–21]. Of note, displays based on μ LEDs are more sustainable than those based on OLEDs because of their superior material stability [16,22]. On the other hand, μ LEDs can also be assembled on a flexible substrate, allowing for wearable display applications [23–25]. However, the full realization of such potential uses of μ LEDs still involves several challenges. Most critically, as illustrated by previous experiments, downsizing LEDs below micron sizes causes a considerable efficiency decrease [26,27]. Significant surface recombination was suggested as an origin of the efficiency drop due to the high surface-to-volume ratio of μ LEDs [28,29]. However, dominant recombination sources that should be identified for optimizing fabrication processes have not yet been clarified.

*youngho84@inu.ac.kr

GaN-based μ LEDs are typically synthesized in one-dimensional (1D) forms, such as wire, rod, and mesa shapes, which are grown along the polar directions of a wurtzite structure [Fig. 1(a)] because of their easy mass production. The planar dimension of these 1D μ LEDs ranges from 0.1×0.1 to $100 \times 100 \mu\text{m}^2$ [30,31]. There are two approaches to obtain 1D μ LED arrays for device fabrication: bottom-up and top-down approaches. In the bottom-up approach, 1D GaN is directly grown on a substrate by using various deposition techniques, such as chemical vapor deposition, metal organic vapor phase epitaxy, and hybrid vapor phase epitaxy [32,33]. For the top-down approach, microscale GaN is first produced by dry and/or wet etching of pregrown bulk GaN, and then it is transferred to predefined areas by assembly techniques [34]. Between the bottom-up and top-down approaches, the latter allows for the easy and quick fabrication of μ LEDs on large wafer scales, and therefore, it is considered to be a suitable method for producing commercial products. However, in the top-down method, the sidewall of μ LEDs, primarily corresponding to the nonpolar (1 $\bar{1}$ 00) m surface of GaN, would be severely damaged during etching processes, generating defective surfaces. According to previous studies, nonstoichiometric Ga-rich or N-rich surfaces were observed after etching processes depending on the process conditions [35–37]. Therefore, large densities of Ga (V_{Ga}) or N (V_{N}) vacancies are expected to be present on the sidewall of μ LEDs. Because these defects may serve as Shockley-Read-Hall (SRH) recombination centers, deteriorating the quantum efficiency of μ LEDs, it is highly desirable to study their impacts on SRH recombination.

First-principles calculations based on density-functional theory (DFT) have been successfully applied to investigate point defects in semiconductors, elucidating the optical and electrical characteristics and chemical stabilities of the defects [38]. Previous DFT calculations demonstrated that the V_{Ga} and V_{N} in bulk GaN cannot be relevant SRH sources because of large formation energies and multiple trap levels (see below) [39–42]. In contrast to bulk defects, surface defects have not been studied thoroughly to date. Huang *et al.* recently reported DFT results on the V_{Ga} on the sidewall of GaN nanowires, suggesting the sidewall V_{Ga} as a recombination center responsible for yellow luminescence [43]. Nayak *et al.* analyzed the energetics of vacancies on the m plane, reporting the V_{N} on the surface as shallow donors [44]. However, the previous results were obtained with generalized gradient approximation (GGA) or local density approximation (LDA) functionals that are not accurate enough to describe the defects of semiconductors because of the band-gap underestimation and charge-delocalization errors [45,46]. Thus, the true nature of the vacancies on the m plane of GaN, especially their impacts on optoelectronic properties, remains elusive.

The foregoing discussion lends urgency to the investigation of the impacts of sidewall V_{Ga} and V_{N} on e - h recombination in GaN μ LEDs. To this end, we scrutinized the energetics and e - h capture characteristics of V_{Ga} and V_{N} on the m plane of GaN using hybrid functional DFT calculations in this study. By analyzing the formation energies of the surface vacancies, we discover that considerable N vacancies can be present on the sidewall of GaN μ LEDs, while the concentration of Ga vacancies would be marginal. In contrast to previous calculations, the surface V_{N} is not a shallow donor. Instead, it develops a deep defect level near the midgap, showing the possibility of capturing both electrons and holes efficiently. The investigation of energetics for electron and hole capture on the surface V_{N} shows that the energy barriers for nonradiative electron and hole capture are small enough to yield high capture coefficients due to strong electron-phonon coupling. Thus, the N vacancies on the sidewall of GaN μ LEDs can work as effective channels for SRH recombination.

II. COMPUTATIONAL DETAILS

Our first-principles calculations are conducted by using the Vienna *ab initio* simulation package (VASP) with projector-augmented wave (PAW) pseudopotentials [47]. The semicore Ga 3d states are treated as valence states. A hybrid functional based on the Heyd-Scuseria-Ernzerhof (HSE06) method is used for the exchange-correlation energy [48]. We select a fraction of the Fock exchange to be 0.29, which produces lattice parameters ($a = 3.18 \text{ \AA}$ and $c = 5.16 \text{ \AA}$) and a band gap (3.50 eV) of bulk GaN consistent with experiments [49–51]. The cutoff energy for the plane-wave basis is set to 500 eV. Throughout this work, spin-polarized calculations are performed. The GaN(1 $\bar{1}$ 00) slab model [Fig. 1(a)] is adopted to simulate the m plane. To avoid interactions between adjacent slabs along the vertical direction due to periodicity, we insert a vacuum with a thickness of 10 \AA . The dangling bonds of the bottom Ga and N atoms are passivated by H atoms with a charge of $1.25e^-$ for Ga and $0.75e^-$ for N. The passivation of the bottom surface is necessary to avoid undesirable interaction between the top and bottom surfaces, which causes errors in calculation results. We did not correct potential changes along the vertical direction that occur in asymmetric slabs. However, we confirm that its correction does not quantitatively affect the results in a meaningful way. For defect calculations, we use $4 \times 4 \times 2$ supercells (128 atoms) for bulk and 3×2 supercells with the five GaN bilayers (132 atoms) for the m surface. We confirm that further increases in slab thickness have little effect on defect properties. A bottom bilayer in the slab is fixed during the atomic relaxation. For the k -point sampling, we use a (0.25, 0.25, 0.25) special k point. The convergence criterion for the atomic force is set to 0.05 eV/ \AA . The defect formation energy (E^f) of a vacancy in the charge state q

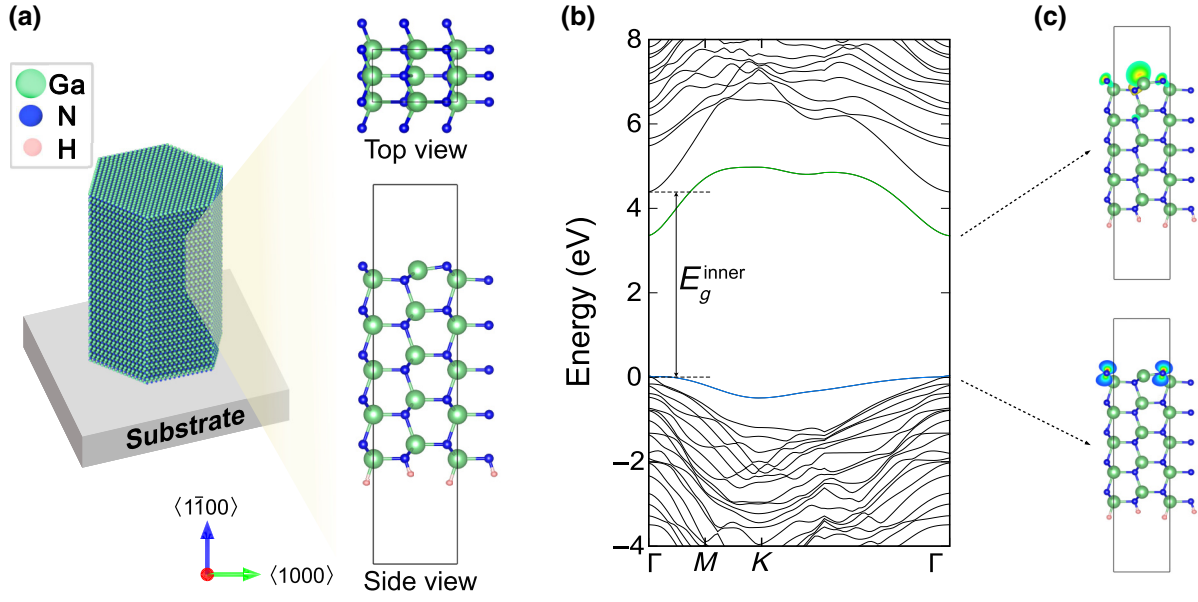


FIG. 1. (a) One-dimensional GaN structure with sidewalls and the slab model for the m plane. (b) Band structure of the slab model for the m plane and (c) charge-density distributions of dangling-bond states at $k = (0.25, 0.25, 0.25)$ (isovalue = $0.012 \text{ e}/\text{\AA}^3$).

(V_i^q where $i = \text{Ga or N}$) [52] is calculated by

$$E^f(V_i^q) = E(V_i^q) - E(\text{perfect}) + \mu_i + qE_F + \Delta^q, \quad (1)$$

where $E(V_i^q)$ and $E(\text{perfect})$ are the total energy of defective and perfect supercells, respectively. μ_i is the chemical potential of Ga or N with respect to that of a stable phase of the corresponding element. We account for $\mu_{\text{Ga}} = 0$ and $\mu_{\text{N}} = \Delta H_f(\text{GaN})$ for Ga-rich conditions and $\mu_{\text{N}} = 0$ and $\mu_{\text{Ga}} = \Delta H_f(\text{GaN})$ for N-rich conditions, where $\Delta H_f(\text{GaN})$ is the heat of formation of GaN. E_F is the Fermi level, i.e., the electron chemical potential. Herein, the reference of E_F is set to the bulk VBM for both bulk and surface defect calculations, which allows for a direct comparison of the formation energies between bulk and surface vacancies. We determine the E_F of the slab with respect to the bulk VBM by aligning the average electrostatic potentials between the clean slab and bulk models, as shown in Fig. S2 within the Supplemental Material [53]. Δ^q is the finite-size correction for charged defects that is obtained using the methods developed by Freysoldt *et al.* (see details about the finite-size correction in Sec. S1 of the Supplemental Material [53]) [54–56].

III. RESULTS AND DISCUSSION

On the m surface, Ga and N atoms form Ga-N dimers [Fig. 1(a)]. The surface Ga atoms shift slightly downward, while the surface N atoms shift upward upon structural

relaxation. Each Ga and N atom on the surface has a single dangling bond, and the electrons in the dangling bonds on the Ga atoms are transferred into those on the N atoms. As a result, the dangling bonds of the Ga (N) atoms generate an empty (occupied) surface state near the conduction- (valence-) band edge, as illustrated in the band structure in Fig. 1(b) and the charge-density distributions in Fig. 1(c). The larger band gap of inner GaN in the slab model (see E_g^{inner} in the band structure) compared to that of the bulk is attributed to the quantum confinement effect (Fig. S3 within the Supplemental Material [53]). With an increase in the slab thickness, we can observe that the N and Ga dangling bond states almost coincide with the bulk VBM and conduction-band minimum (CBM), respectively.

The rate of SRH recombination on a given defect that involves successive electron and hole captures strongly depends on the position of the defect states. Technically, these defect states correspond to charge transition levels between two successive charge states $\epsilon(q/q')$, which are defined as the Fermi-level position at which a transition of the relative stability between two different charge states occurs. An electron (hole) tends to be captured by a defect faster in a nonradiative manner when the defect level approaches the conduction- (valence-) band edge, while a hole- (electron-) capture process becomes slower. This trend indicates that the defect with a level close to midgap can be an effective SRH recombination center because it can efficiently capture both electrons and holes. If a defect has multiple defect levels, the defect is likely to be trapped in a specific charge state associated with the transition level

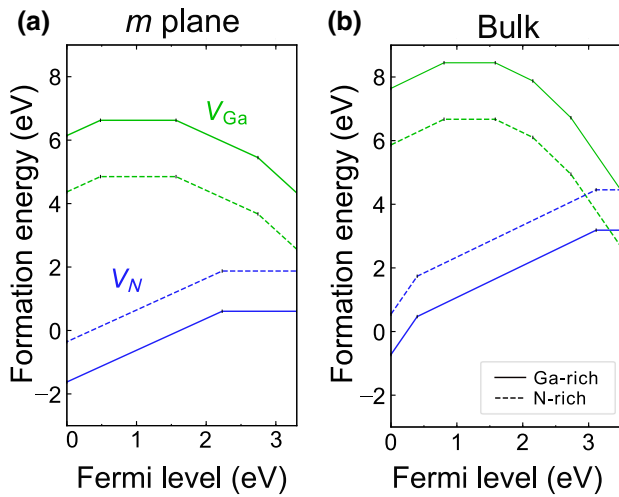


FIG. 2. Formation energies of the Ga and N vacancies (a) on the m plane and (b) in the bulk as a function of the Fermi level at the Ga-rich and N-rich limits.

relatively close to the band extrema. As a result, multilevel defects with defect levels near the band edges are unlikely to be critical for SRH recombination [57].

Figure 2(a) shows the formation energies of V_{Ga} and V_{N} on the m surface, hereafter called $V_{\text{Ga,surf}}$ and $V_{\text{N,surf}}$, respectively (the atomic configurations are provided in Fig. S5 within the Supplemental Material [53]). For comparative purposes, we also present the formation energies of bulk V_{Ga} and V_{N} , hereafter called $V_{\text{Ga,bulk}}$ and $V_{\text{N,bulk}}$, respectively, in Fig. 2(b). We provide only the formation energy for the most stable charge state of a defect while the Fermi level varies between the band gap, and it is expressed as a slope of a formation energy curve. The calculated vacancy formation energies for the bulk are highly consistent with previous calculations. We find that $V_{\text{Ga,surf}}$ can be present in several different charge states as $V_{\text{Ga,bulk}}$, developing $\epsilon(+/0)$ and $\epsilon(-/2-)$ near the valence and conduction bands, respectively. As a result, the SRH recombination on $V_{\text{Ga,surf}}$ would not be efficient. Moreover, the formation energy of $V_{\text{Ga,surf}}$ is still too large for the concentration of $V_{\text{Ga,surf}}$ to be significant enough to have a critical effect on the SRH recombination when (sub)micro-sized GaN is under thermal equilibrium.

The large formation energy also implies that most of the excess Ga vacancies that can be created by etching processes in top-down approaches to obtain a μ LED array are likely to be annihilated during postannealing or fabrication processes. Therefore, $V_{\text{Ga,surf}}$ alone is not expected to serve as a critical SRH recombination center. However, as $V_{\text{Ga,bulk}}$ does, some excess Ga vacancies may be retained by forming more stable defect complexes with other impurities, such as carbon, oxygen, and/or hydrogen, and these defect complexes would undermine the optoelectronic properties of GaN [58–60].

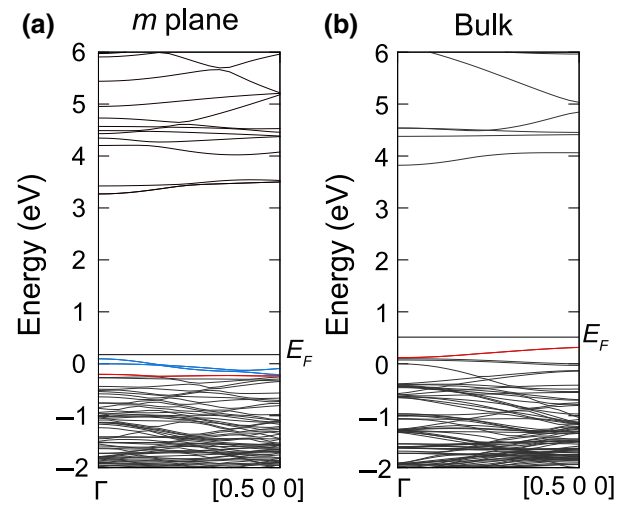


FIG. 3. Band structures of V_{N}^+ (a) on the m plane and (b) in the bulk. The occupied defect state is colored in red. The VBM and surface state derived by the N dangling bonds are colored in blue.

Notably, $V_{\text{N,surf}}$ is found to behave differently from $V_{\text{N,bulk}}$ in three respects. (The orbital characteristics of single-particle states for $V_{\text{N,surf}}$ and $V_{\text{N,bulk}}$ can be found in the Supplemental Material [53].) First, $V_{\text{N,surf}}$ develops only a single transition level $\epsilon(+/0)$ inside the band gap, while $V_{\text{N,bulk}}$ generates multiple transition levels. $V_{\text{N,bulk}}^{2+}$ is relatively unstable, and the transition levels $\epsilon(3+/2+)$ and $\epsilon(2+/+)$ near VBM+0.40 eV are not marked in Fig. 2(a). The absence of $\epsilon(3+/2+)$ and $\epsilon(2+/+)$ in the $V_{\text{N,surf}}$ between the band gap arises from the fact that the occupied electronic states of $V_{\text{N,surf}}^+$ lie below the VBM, as shown in Fig. 3(a). Therefore, it is energetically unfavorable for $V_{\text{N,surf}}^{2+}$ and $V_{\text{N,surf}}^{3+}$ to be formed by capturing more holes. In contrast, the occupied defect levels of $V_{\text{N,bulk}}^+$ for capturing holes are present above the VBM in bulk [Fig. 3(b)].

Second, the $\epsilon(+/0)$ position of $V_{\text{N,surf}}$ (VBM+2.2 eV) is deeper in energy than that of $V_{\text{N,bulk}}$ (VBM+3.1 eV). This result can be attributed to the smaller N^{3-} coordination of surface Ga ions compared to that for bulk Ga ions; the surface Ga sites have higher electrostatic potential so that the overlap between empty $4s$ states of the neighboring Ga ions of $V_{\text{N,surf}}$ can produce defect states with lower energies. This allows $V_{\text{N,bulk}}^0$ to be stable over a wider range of the Fermi level compared to $V_{\text{N,bulk}}^0$. Unlike $V_{\text{N,bulk}}$, the single, deep defect level of $V_{\text{N,surf}}$ close to the midgap region may indicate that $V_{\text{N,surf}}$ plays a role as a SRH recombination center. This finding will be confirmed by constructing the so-called configuration-coordinate diagram (CC diagram) below.

Lastly, the formation energy of $V_{\text{N,surf}}$ is small, between 0 and 2 eV, depending on the growth conditions. Therefore, the concentration of surface N vacancies is expected

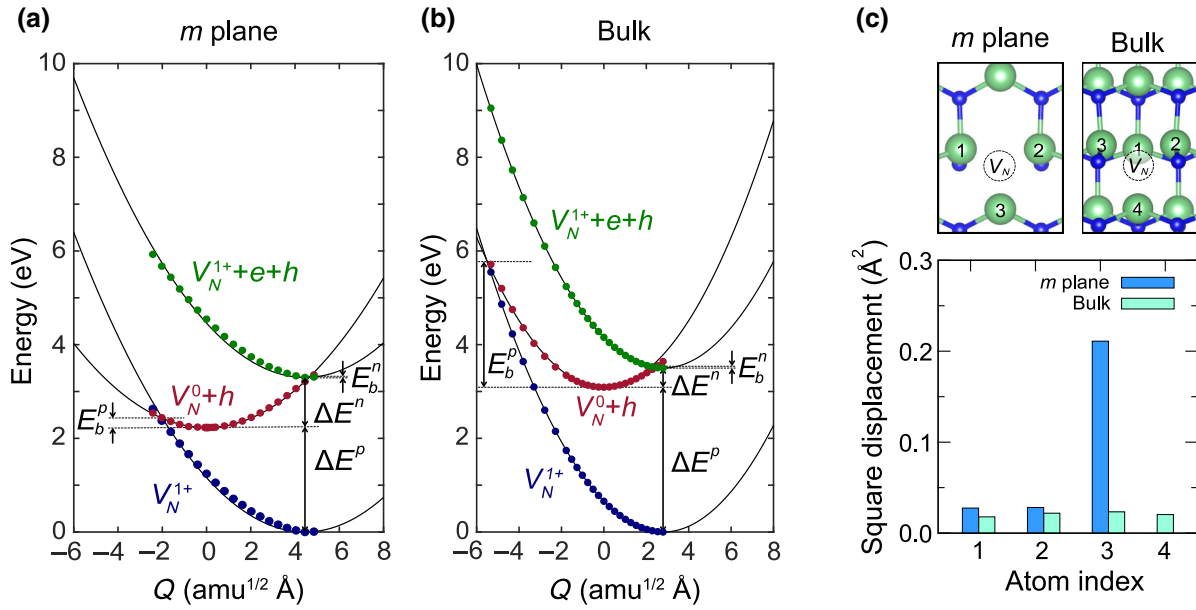


FIG. 4. Configuration-coordinate diagrams for electron and hole capture processes on (a) surface and (b) bulk V_N . The lines are second-order fit to the calculation data. (c) Atomic structure of surface and bulk V_N in the neutral state, and square displacements of neighboring Ga atoms around V_N due to the transition of the charge state from $q = 0$ to $1+$.

to be significant even if synthesized GaN is thermally equilibrated. Interestingly, recent electron energy loss spectroscopy (EELS) measurements on GaN nanostructures grown by molecular beam epitaxy showed strong subgap absorption at 2.2 eV [44]. The absorption energy coincides with the optical transition energy of 2.31 eV for $V_{N,\text{surf}}^0 \rightarrow V_{N,\text{surf}}^{1+} + e^-$ (Fig. S7 within the Supplemental Material [53]). This consistency would manifest an abundance of surface N vacancies. More recently, Sagisaka *et al.* directly visualized surface N vacancies using scanning tunneling microscopy and atomic force microscopy [61]. On the other hand, the E^f of $V_{N,\text{surf}}$ is approximately 1 eV smaller than that of $V_{N,\text{bulk}}$. Thus, nitrogen vacancies below the *m* surface that can be generated by etching damage in top-down processes would diffuse out to the surface and accumulate, boosting SRH recombination.

To corroborate the negative impacts of V_N on SRH recombination, we build the CC diagram describing electron and hole capture into $\epsilon(+/0)$, as shown in Fig. 4(a) for $V_{N,\text{surf}}$ and Fig. 4(b) for $V_{N,\text{bulk}}$. Q is the generalized configuration coordinate defined by the total mass-weighted distortion of the atomic structure with respect to that of V_N in the neutral state. The transition energy of $\Delta E^{n(p)}$ for electron (hole) capture, which is also referred to as the zero-phonon line in the optical transition, is determined by the $\epsilon(+/0)$ position relative to the CBM (VBM). The sum of $\Delta E^n + \Delta E^p$ corresponds to the band gap of GaN. A complete SRH recombination cycle consists of two successive capture processes: electron capture by the V_N in the $1+$ state, followed by hole capture by the V_N in the neutral

state. $E_b^{n(p)}$ is the energy barrier for nonradiative capture of an electron (hole). Considering the quantum tunneling effect, the energy barrier can decrease. Because of the exponential dependence of the capture cross section on the energy barrier [62], the slower process with a higher barrier between electron and hole capture processes is likely to dominate the overall recombination rate on a single defect site.

For $V_{N,\text{surf}}$, hole capture gives rise to a higher capture barrier of 0.27 eV than that for the electron capture of 0.03 eV being the rate-determining step, as inferred by the position of $\epsilon(+/0)$. According to previous calculations, Ca substituting Ga (Ca_{Ga}) in $\text{In}_x\text{Ga}_{1-x}\text{N}$ leads to a similar hole-capture barrier for In-rich compositions, resulting in a significant capture coefficient [63]. When examining the capture coefficient using *nonrad* code [64], we indeed find a significant value of $2 \times 10^{-7} \text{ cm}^3/\text{s}$ that is higher than approximately $2 \times 10^{-9} \text{ cm}^3/\text{s}$ for hole capture on Ca_{Ga} and comparable to approximately $1 \times 10^{-7} \text{ cm}^3/\text{s}$ for electron capture on $V_{\text{Ga-3H}}$ in $\text{In}_x\text{Ga}_{1-x}\text{N}$ [57,63]. (The temperature is set to 390 K that is a typical operating temperature of LED.) Therefore, $V_{N,\text{surf}}$ is likely to work as an effective SRH recombination center that deteriorates the quantum efficiency of μLEDs . On the other hand, as in $V_{N,\text{surf}}$, the harder (easier) capture of a hole (electron) is also expected from the position of $\epsilon(+/0)$ for $V_{N,\text{bulk}}$. However, the E_b^p for $V_{N,\text{bulk}}$ (2.6 eV) is even larger than that for $V_{N,\text{surf}}$, resulting in a negligible capture coefficient of approximately $10^{-30} \text{ cm}^3/\text{s}$. As a result, $V_{N,\text{bulk}}$

cannot act as a critical SRH center. The much lower E_b^p for $V_{N,\text{surf}}$ compared to that for $V_{N,\text{bulk}}$ partly relates to the lower position of $\epsilon(+/0)$ in the former. Another reason for the smaller E_b^p is the stronger electron-phonon coupling of $V_{N,\text{surf}}$ compared to that of $V_{N,\text{bulk}}$, as evidenced by larger Huang-Rhys factors that quantify electron-phonon interactions (Table S1 within the Supplemental Material [53]) [65,66]. Specifically, atomic distortion upon electron or hole capture, namely the ΔQ of $V_{N,\text{surf}}$ is greater than that of $V_{N,\text{bulk}}$, and thus, hole capture on $V_{N,\text{surf}}$ becomes facile. The analysis of atom-resolved ΔQ^2 in Fig. 4(c) shows that the strong electron-phonon interaction of $V_{N,\text{surf}}$ is associated with the Ga ion at the top surface; the Ga ion lacks a Ga-N bond (Fig. S8 within the Supplemental Material [53]) such that it can displace significantly during carrier capture. Meanwhile, displacements of the four neighboring Ga ions of $V_{N,\text{bulk}}$ are smaller and similarly contribute to total structural distortion.

According to our results, synthesis techniques that can prevent the formation of surface V_N are advantageous for the efficiency of μ LEDs. Indeed, it was demonstrated that high-temperature (approximately 700 °C) annealing in air or N_2 atmosphere for longer than the typical annealing time recovers the sidewall damages of GaN pillars induced by etching and enhances the internal quantum efficiency of LEDs [67,68]. In addition, sidewall passivation using AlN, which may work as a nitrogen source, was recently reported to be effective in eliminating SRH recombination centers on the sidewall of GaN μ LEDs [69].

IV. CONCLUSIONS

Using hybrid DFT calculations, we investigate the V_N and V_{Ga} on the GaN m surface. From the formation-energy diagram, we illustrate that the concentration of V_{Ga} would be low and that the surface V_{Ga} is unlikely to provide effective channels for SRH recombination. In contrast, a sizable amount of V_N can be present on the m plane, and this surface V_N produces a deep level near the midgap. With the CC diagram, we corroborate that the energy barriers for electron and hole capture on the surface V_N are small enough to give rise to large capture coefficients because of strong electron-phonon coupling. Our results support the recent experimental observation that GaN with nitrogen vacancies on the sidewall created during the etching process yields inferior device performances if an adequate post-treatment of the sidewall is not applied [70]. By providing a detailed analysis of the atomic and electronic structures of the surface vacancies as well as enlightening their impacts on SRH recombination, this study will pave the way to developing next-generation displays and optoelectronic devices based on GaN μ LEDs.

ACKNOWLEDGMENTS

This research is supported by Samsung Display Co., LTD. The computation is performed at Korea Institute of Science and Technology Information (KISTI) National Supercomputing Center (KSC-2020-CRE-0296).

- [1] M. Schadt, Milestone in the history of Field-Effect liquid crystal displays and materials, *Jpn. J. Appl. Phys.* **48**, 03B001 (2009).
- [2] H. Sasabe, H. Nakanishi, Y. Watanabe, S. Yano, M. Hirasawa, Y.-J. Pu, and J. Kido, Extremely low operating voltage green phosphorescent organic light-emitting devices, *Adv. Funct. Mater.* **23**, 5550 (2013).
- [3] K.-H. Kim, S. Lee, C.-K. Moon, S.-Y. Kim, Y.-S. Park, J.-H. Lee, J. W. Lee, J. Huh, Y. You, and J.-J. Kim, Phosphorescent dye-based supramolecules for high-efficiency organic light-emitting diodes, *Nat. Commun.* **5**, 4769 (2014).
- [4] J.-H. Lee, C.-H. Chen, P.-H. Lee, H.-Y. Lin, M.-K. Leung, T.-L. Chiu, and C.-F. Lin, Blue organic light-emitting diodes: Current status, challenges, and future outlook, *J. Mater. Chem.* **7**, 5874 (2019).
- [5] Y. Huang, E.-L. Hsiang, M.-Y. Deng, and S.-T. Wu, Mini-LED, micro-LED and OLED displays: Present status and future perspectives, *Light Sci. Appl.* **9**, 105 (2020).
- [6] J. B. Son, J. Kang, S. Bae, K. Y. Yang, J. Han, K. S. Min, C. Lee, S. Sul, and S. K. Kim, Discrimination of degradation mechanisms for organic light-emitting diodes by in situ, Layer-Specific spectroscopic analysis, *ACS Photonics* **9**, 82 (2022).
- [7] T. Zhan, K. Yin, J. Xiong, Z. He, and S.-T. Wu, Augmented reality and virtual reality displays: Perspectives and challenges, *iScience* **23**, 101397 (2020).
- [8] S. Hang, C.-M. Chuang, Y. Zhang, C. Chu, K. Tian, Q. Zheng, T. Wu, Z. Liu, Z.-H. Zhang, Q. Li, and H.-C. Kuo, A review on the low external quantum efficiency and the remedies for GaN-based micro-LEDs, *J. Phys. D Appl. Phys.* **54**, 153002 (2021).
- [9] S. Nakamura, Current status of GaN-based solid-state lighting, *MRS Bull.* **34**, 101 (2009).
- [10] J. Simon, V. Protasenko, C. Lian, H. Xing, and D. Jena, Polarization-induced hole doping in wide-band-gap uniaxial semiconductor heterostructures, *Science* **327**, 60 (2010).
- [11] S. Nakamura and M. R. Krames, History of gallium-nitride-based light-emitting diodes for illumination, *Proc. IEEE* **101**, 2211 (2013).
- [12] J. H. Choi, A. Zoulkarneev, S. I. Kim, C. W. Baik, M. H. Yang, S. S. Park, H. Suh, U. J. Kim, H. Bin Son, J. S. Lee, M. Kim, J. M. Kim, and K. Kim, Nearly single-crystalline GaN light-emitting diodes on amorphous glass substrates, *Nat. Photonics* **5**, 763 (2011).
- [13] H. S. Wasisto, J. D. Prades, J. Gülink, and A. Waag, Beyond solid-state lighting: Miniaturization, hybrid integration, and applications of GaN nano- and micro-LEDs, *Appl. Phys. Rev.* **6**, 041315 (2019).
- [14] P. P. Iyer, R. A. DeCrescent, Y. Mohtashami, G. Lheureux, N. A. Butakov, A. Alhassan, C. Weisbuch, S. Nakamura,

- S. P. DenBaars, and J. A. Schuller, Unidirectional luminescence from InGaN/GaN quantum-well metasurfaces, *Nat. Photonics* **14**, 543 (2020).
- [15] S.-I. Park, Y. Xiong, R.-H. Kim, P. Elvikis, M. Meitl, D.-H. Kim, J. Wu, J. Yoon, C.-J. Yu, Z. Liu, Y. Huang, K.-C. Hwang, P. Ferreira, X. Li, K. Choquette, and J. A. Rogers, Printed assemblies of inorganic light-emitting diodes for deformable and semitransparent displays, *Science* **325**, 977 (2009).
- [16] J. Day, J. Li, D. Y. C. Lie, C. Bradford, J. Y. Lin, and H. X. Jiang, III-nitride full-scale high-resolution microdisplays, *Appl. Phys. Lett.* **99**, 031116 (2011).
- [17] J. B. Park, W. S. Choi, T. H. Chung, S. H. Lee, M. K. Kwak, J. S. Ha, and T. Jeong, Transfer printing of vertical-type microscale light-emitting diode array onto flexible substrate using biomimetic stamp, *Opt. Express* **27**, 6832 (2019).
- [18] J. Park, J. H. Choi, K. Kong, J. H. Han, J. H. Park, N. Kim, E. Lee, D. Kim, J. Kim, D. Chung, S. Jun, M. Kim, E. Yoon, J. Shin, and S. Hwang, Electrically driven mid-submicrometre pixelation of InGaN micro-light-emitting diode displays for augmented-reality glasses, *Nat. Photonics* **15**, 449 (2021).
- [19] K. Zhang, D. Peng, K. M. Lau, and Z. Liu, Fully-integrated active matrix programmable UV and blue micro-LED display system-on-panel (SoP), *J. Soc. Inf. Disp.* **25**, 240 (2017).
- [20] L. Zhang, F. Ou, W. C. Chong, Y. Chen, Y. Zhu, and Q. Li, 31.1: Invited paper: Monochromatic active matrix micro-LED micro-displays with > 5, 000 dpi pixel density fabricated using monolithic hybrid integration process, *Dig. Tech. Papers* **49**, 333 (2018).
- [21] F. Gou, E.-L. Hsiang, G. Tan, Y.-F. Lan, C.-Y. Tsai, and S.-T. Wu, High performance color-converted micro-LED displays, *J. Soc. Inf. Disp.* **27**, 199 (2019).
- [22] G. Chen, M. Craven, A. Kim, A. Munkholm, S. Watanabe, M. Camras, W. Götz, and F. Steranka, Performance of high-power III-nitride light emitting diodes, *Phys. Status Solidi* **205**, 1086 (2008).
- [23] Y. C. Chiang, C. C. Lin, and H. C. Kuo, Novel thin-GaN LED structure adopted micro abraded surface to compare with conventional vertical LEDs in ultraviolet light, *Nanoscale Res. Lett.* **10**, 182 (2015).
- [24] B. Hahn, B. Galler, and K. Engl, Development of high-efficiency and high-power vertical light emitting diodes, *Jpn. J. Appl. Phys.* **53**, 100208 (2014).
- [25] P. Tian, J. J. D. McKendry, E. Gu, Z. Chen, Y. Sun, G. Zhang, M. D. Dawson, and R. Liu, Fabrication, characterization and applications of flexible vertical InGaN micro-light emitting diode arrays, *Opt. Express* **24**, 699 (2016).
- [26] M. S. Wong, D. Hwang, A. I. Alhassan, C. Lee, R. Ley, S. Nakamura, and S. P. DenBaars, High efficiency of III-nitride micro-light-emitting diodes by sidewall passivation using atomic layer deposition, *Opt. Express* **26**, 21324 (2018).
- [27] K. Ding, V. Avrutin, N. Izyumskaya, Ü. Özgür, and H. Morkoç, Micro-LEDs, a manufacturability perspective, *NATO Adv. Sci. Inst. Ser. E Appl. Sci.* **9**, 1206 (2019).
- [28] F. Olivier, A. Daami, C. Licitra, and F. Templier, Shockley-Read-Hall and auger non-radiative recombination in GaN based LEDs: A size effect study, *Appl. Phys. Lett.* **111**, 022104 (2017).
- [29] J. Kou, C.-C. Shen, H. Shao, J. Che, X. Hou, C. Chu, K. Tian, Y. Zhang, Z.-H. Zhang, and H.-C. Kuo, Impact of the surface recombination on InGaN/GaN-based blue micro-light emitting diodes, *Opt. Express* **27**, A643 (2019).
- [30] E. D. Le Boulbar, C. J. Lewins, D. W. E. Allsopp, C. R. Bowen, and P. A. Shields, Fabrication of high-aspect ratio GaN nanostructures for advanced photonic devices, *Microelectron. Eng.* **153**, 132 (2016).
- [31] H. K. Park, S. W. Yoon, Y. J. Eo, W. W. Chung, G. Y. Yoo, J. H. Oh, K. N. Lee, W. Kim, and Y. R. Do, Horizontally assembled green InGaN nanorod LEDs: Scalable polarized surface emitting LEDs using electric-field assisted assembly, *Sci. Rep.* **6**, 28312 (2016).
- [32] T. Kuykendall, P. Pauzuskie, S. Lee, Y. Zhang, J. Goldberger, and P. Yang, Metalorganic chemical vapor deposition route to GaN nanowires with triangular cross sections, *Nano Lett.* **3**, 1063 (2003).
- [33] F. A. Ponce and D. P. Bour, Nitride-based semiconductors for blue and green light-emitting devices, *Nature* **386**, 351 (1997).
- [34] Q. Li, K. R. Westlake, M. H. Crawford, S. R. Lee, D. D. Koleske, J. J. Figiel, K. C. Cross, S. Fatholouloumi, Z. Mi, and G. T. Wang, Optical performance of top-down fabricated InGaN/GaN nanorod light emitting diode arrays, *Opt. Express* **19**, 25528 (2011).
- [35] E. Despiau-Pujo and P. Chabert, MD simulations of GaN sputtering by Ar⁺ ions: Ion-induced damage and near-surface modification under continuous bombardment, *J. Vac. Sci. Technol. A* **28**, 1105 (2010).
- [36] H.-S. Kim, G.-Y. Yeom, J.-W. Lee, and T.-I. Kim, A study of GaN etch mechanisms using inductively coupled Cl₂/Ar plasmas, *Thin Solid Films* **341**, 180 (1999).
- [37] Y.-H. Lai, C.-T. Yeh, J.-M. Hwang, H.-L. Hwang, C.-T. Chen, and W.-H. Hung, Sputtering and etching of GaN surfaces, *J. Phys. Chem. B* **105**, 10029 (2001).
- [38] N. Sanders, D. Bayerl, G. Shi, K. A. Mengle, and E. Kioupakis, Electronic and optical properties of two-dimensional GaN from first-principles, *Nano Lett.* **17**, 7345 (2017).
- [39] J. L. Lyons, D. Wickramaratne, and C. G. Van de Walle, A first-principles understanding of point defects and impurities in GaN, *J. Appl. Phys.* **129**, 111101 (2021).
- [40] J. L. Lyons and C. G. Van de Walle, Computationally predicted energies and properties of defects in GaN, *npj Comput. Mater.* **3**, 1 (2017).
- [41] G. Miceli and A. Pasquarello, Energetics of native point defects in GaN: A density-functional study, *Microelectron. Eng.* **147**, 51 (2015).
- [42] I. C. Diallo and D. O. Demchenko, Native Point Defects in GaN: A Hybrid-Functional Study, *Phys. Rev. Appl.* **6**, 064002 (2016).
- [43] P. Huang, H. Zong, J.-J. Shi, M. Zhang, X.-H. Jiang, H.-X. Zhong, Y.-M. Ding, Y.-P. He, J. Lu, and X.-D. Hu, Origin of 3.45 eV emission line and yellow luminescence band in GaN nanowires: Surface microwire and defect, *ACS Nano* **9**, 9276 (2015).
- [44] S. Nayak, M. H. Naik, M. Jain, U. V. Waghmare, and S. M. Shivaprasad, First-principles theoretical analysis and

- electron energy loss spectroscopy of vacancy defects in bulk and nonpolar (10 $\bar{1}$ 0) surface of GaN, *J. Vac. Sci. Technol. A* **38**, 063205 (2020).
- [45] J. Heyd and G. E. Scuseria, Efficient hybrid density functional calculations in solids: Assessment of the Heyd-Scuseria-Ernzerhof screened Coulomb hybrid functional, *J. Chem. Phys.* **121**, 1187 (2004).
- [46] A. Janotti, J. B. Varley, P. Rinke, N. Umezawa, G. Kresse, and C. G. Van de Walle, Hybrid functional studies of the oxygen vacancy in TiO₂, *Phys. Rev. B Condens. Matter Mater. Phys.* **81**, 085212 (2010).
- [47] G. Kresse and J. Furthmüller, Efficiency of ab-initio total energy calculations for metals and semiconductors using a plane-wave basis set, *Comput. Mater. Sci.* **6**, 15 (1996).
- [48] J. Heyd, G. E. Scuseria, and M. Ernzerhof, Hybrid functionals based on a screened Coulomb potential, *J. Chem. Phys.* **118**, 8207 (2003).
- [49] H. Morkoc, *Handbook of Nitride Semiconductors and Devices: GaN-Based Optical and Electronic Devices: Vol. 3: GaN-Based Optical and Electronic Devices*, Handbook of Nitride Semiconductors and Devices (Vch) (Wiley-VCH Verlag, Weinheim, Germany, 2008)
- [50] R. Dingle, D. D. Sell, S. E. Stokowski, and M. Ilegems, Absorption, reflectance, and luminescence of GaN epitaxial layers, *Phys. Rev. B* **4**, 1211 (1971).
- [51] B. Monemar, Fundamental energy gap of GaN from photoluminescence excitation spectra, *Phys. Rev. B Condens. Matter* **10**, 676 (1974).
- [52] C. Freysoldt, B. Grabowski, T. Hickel, J. Neugebauer, G. Kresse, A. Janotti, and C. G. Van de Walle, First-principles calculations for point defects in solids, *Rev. Mod. Phys.* **86**, 253 (2014).
- [53] See Supplemental Material at <http://link.aps.org/supplemental/10.1103/PhysRevApplied.19.014018> for detailed explanation of specific Freysoldt correction schemes in a GaN system with vacancy, convergence tests for formation energies with the Freysoldt correction scheme, band-alignment schematics, the band structures over different bilayers, potential profiles for the correction term of the defect formation energy, atomic structures with vacancies, charge distributions of a surface and bulk nitrogen vacancy, schematic configurational coordination diagram of N vacancy on surface, atomic structure of the *m* surface with V_N^+ at the top surface, and effective parameters for N vacancy related to the luminescence transition in GaN.
- [54] C. Freysoldt, J. Neugebauer, and C. G. Van de Walle, Fully Ab Initio Finite-Size Corrections for Charged-Defect Supercell Calculations, *Phys. Rev. Lett.* **102**, 016402 (2009).
- [55] C. Freysoldt, J. Neugebauer, and C. G. Van de Walle, Electrostatic interactions between charged defects in supercells, *Phys. Status Solidi B Basic Res.* **248**, 1067 (2011).
- [56] C. Freysoldt and J. Neugebauer, First-principles calculations for charged defects at surfaces, interfaces, and two-dimensional materials in the presence of electric fields, *Phys. Rev. B Condens. Matter* **97**, 205425 (2018).
- [57] C. E. Dreyer, A. Alkauskas, J. L. Lyons, J. S. Speck, and C. G. Van de Walle, Gallium vacancy complexes as a cause of Shockley-Read-Hall recombination in III-nitride light emitters, *Appl. Phys. Lett.* **108**, 141101 (2016).
- [58] J. Neugebauer and C. G. Van de Walle, Gallium vacancies and the yellow luminescence in GaN, *Appl. Phys. Lett.* **69**, 503 (1996).
- [59] D. O. Demchenko, I. C. Diallo, and M. A. Reshchikov, Yellow Luminescence of Gallium Nitride Generated by Carbon Defect Complexes, *Phys. Rev. Lett.* **110**, 087404 (2013).
- [60] M. A. Reshchikov, D. O. Demchenko, A. Usikov, H. Helava, and Y. Makarov, Carbon defects as sources of the green and yellow luminescence bands in undoped GaN, *Phys. Rev. B Condens. Matter* **90**, 235203 (2014).
- [61] K. Sagisaka, O. Custance, N. Ishida, T. Nakamura, and Y. Koide, Identification of a nitrogen vacancy in GaN by scanning probe microscopy, *Phys. Rev. B* **106**, 115309 (2022).
- [62] A. M. Stoneham, *Theory of Defects in Solids: Electronic Structure of Defects in Insulators and Semiconductors* (Clarendon Press, New York, 2001).
- [63] J.-X. Shen, D. Wickramaratne, C. E. Dreyer, A. Alkauskas, E. Young, J. S. Speck, and C. G. Van de Walle, Calcium as a nonradiative recombination center in InGa_N, *Appl. Phys. Express* **10**, 021001 (2017).
- [64] M. E. Turiansky, A. Alkauskas, M. Engel, G. Kresse, D. Wickramaratne, J.-X. Shen, C. E. Dreyer, and C. G. Van de Walle, Nonrad: Computing nonradiative capture coefficients from first principles, *Comput. Phys. Commun.* **267**, 108056 (2021).
- [65] K. Huang, A. Rhys, and N. F. Mott, Theory of light absorption and non-radiative transitions in f-centres, *Proc. R. Soc. Lond. A Math. Phys. Sci.* **204**, 406 (1950).
- [66] A. Alkauskas, Q. Yan, and C. G. Van de Walle, First-principles theory of nonradiative carrier capture via multiphonon emission, *Phys. Rev. B* **90**, 075202 (2014).
- [67] P. Tian, J. J. D. McKendry, Z. Gong, B. Guilhabert, I. M. Watson, E. Gu, Z. Chen, G. Zhang, and M. D. Dawson, Size-dependent efficiency and efficiency droop of blue InGa_N micro-light emitting diodes, *Appl. Phys. Lett.* **101**, 231110 (2012).
- [68] A. Y. Polyakov, L. A. Alexanyan, M. L. Skorikov, A. V. Chernykh, I. V. Shchemerov, V. N. Murashev, T.-H. Kim, I.-H. Lee, and S. J. Pearton, Post dry etching treatment of nanopillar GaN/InGa_N multi-quantum-wells, *J. Alloys Compd.* **868**, 159211 (2021).
- [69] D. Chen, Z. Wang, F.-C. Hu, C. Shen, N. Chi, W. Liu, D. W. Zhang, and H.-L. Lu, Improved electro-optical and photoelectric performance of GaN-based micro-LEDs with an atomic layer deposited AlN passivation layer, *Opt. Express* **29**, 36559 (2021).
- [70] G. M. Foster, A. Koehler, M. Ebrish, J. Gallagher, T. Anderson, B. Noesges, L. Brillson, B. Gunning, K. D. Hobart, and F. Kub, Recovery from plasma etching-induced nitrogen vacancies in *p*-type gallium nitride using UV/O₃ treatments, *Appl. Phys. Lett.* **117**, 082103 (2020).